

Relative Ages of Globular Clusters

Thomas H. Puzia¹

Sternwarte der Universität München, Scheinerstrasse 1, D-81679 München, Germany

Abstract. Ages of extragalactic globular clusters can provide valuable insights into the formation and evolution of galaxies. In this contribution the photometric methods of age dating old globular cluster systems are summarised. The spectroscopic approach is reviewed with an emphasis of the right choice of age diagnostics. We present a new method of quantifying the relatively best age-sensitive spectroscopic index given the quality of a data set and a certain theoretical stellar synthesis model. The relatively best diagnostic plot is constructed from the set of Lick indices and used to age date globular clusters in several early-type galaxies which are part of a large spectroscopic survey of extragalactic globular cluster systems. We find that, independently of host galaxy, metal-poor ($[\text{Fe}/\text{H}] < -0.8$) globular clusters appear to be old ($t > 8$ Gyr) and coeval. Metal-rich clusters show a wide range of ages from ~ 15 down to a few Gyr.

1 Introduction

The foundation of understanding galaxy formation and evolution is the access to accurate ages of stellar populations which build up galaxies. All galaxies are expected to host multiple stellar populations with different ages, but it is uncertain when and how they formed. In general, the ages of galaxies are determined from photometric and/or spectroscopic parameters which are more or less correlated with the mean lifetime of the observed stellar system. Looking at the diffuse light of galaxies one observes the luminosity-weighted sum of all contributions emitted by a mix of stellar populations with various ages. Hence, it is meaningless to assign a single age to galaxies and impossible to resolve the age spread of the underlying stellar populations by looking at the diffuse light alone.

In the recent past, globular clusters increasingly played the role of accurate age tracers. Globular clusters are simple stellar populations (SSPs, containing stars of same age and same metallicity), are formed during major star formation events, and are easy to observe out to large distances. The easy age dating of these witnesses of galaxy evolution makes it possible to assign single star-burst events to globular cluster sub-populations and thus reconstruct the star formation histories of galaxies. However, there are still fundamental limits of accurate age dating: (1) photometric and spectroscopic age diagnostics suffer from the well-known age-metallicity degeneracy and (2) stochastic fluctuations in bright stellar evolutionary phases in less-massive clusters ($\leq 10^5 M_\odot$) limit the accuracy of age determinations. The remedy for the former point is a smart choice of photometric colours and/or spectroscopic indices to reduce the age-

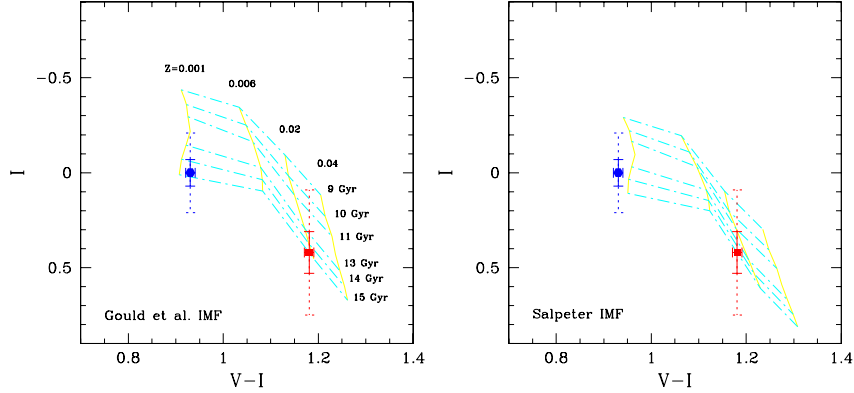


Fig. 1. Age dating of globular clusters in NGC 4472 taken from [7]. The dots indicate the colours and turn-over magnitudes of the two major globular cluster sub-populations which are compared to the SSP model predictions. Different CMD and SSP models variations were analysed and gave very similar results. The two globular cluster sub-populations were found to differ mainly in metallicity. For details see [7]

metallicity degeneracy. The latter problem can be by-passed by averaging over a large sample of globular clusters.

In the following, the two fundamental techniques of age dating of old globular clusters are discussed. We will focus on globular cluster systems which are older than 1 Gyr and hosted in early-type galaxies. Finally, first results of our spectroscopic survey of extragalactic globular cluster systems are presented.

2 Photometric Age Dating

Photometric ages of extragalactic globular clusters are obtained from the comparison of observed parameters with theoretical model predictions. Such models are calibrated on Local Group globular clusters for which the ages are known from other techniques. However, the globular clusters in the Local Group are not always representative for the variety of clusters found outside the Local Group, e.g. in early-type galaxies. To obtain meaningful results for clusters with high metallicities which cannot be observed locally one uses extrapolations to derive their ages. Absolute age predictions vary among SSP models as they depend on the ingredients of the model and the choice of local calibrators. It is essential to use more than one model when accurate absolute ages are required to secure oneself from model-to-model variations. However, relative ages can be reliably obtained using any SSP model as the differential predictions are less affected by the choice of a specific model. Photometric age dating methods use colour-magnitude diagrams (CMDs) and colour-colour diagrams as their tools.

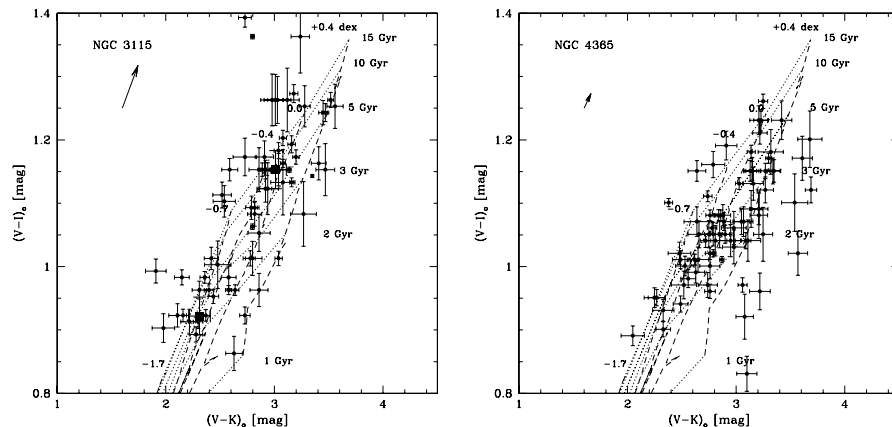


Fig. 2. $(V - I)$ vs. $(V - K)$ diagnostic plots for globular clusters in NGC 3115 (*left panel*) and NGC 4365 (*right panel*) taken from [8]. A significant intermediate-age globular cluster sub-population is detected in NGC 4365. All used SSP models indicate that these objects have age between 2 and 8 Gyr and metallicities $\sim 0.5Z_{\odot} - 3Z_{\odot}$. See contribution of Hempel et al. (this volume) and [3] for further systems

2.1 Colour-Magnitude Method

The first method is based on mean colours and turn-over magnitudes of major globular cluster sub-populations. The requirement is that the sub-populations can be separated by their colours and their luminosity function turn-over magnitudes can be observed. In other words, this method is only applicable to old globular cluster systems with “evolved” globular cluster luminosity functions. An application is shown in Figure 1 where relative ages of the two major globular cluster sub-populations in NGC 4472 can be read off directly from the model grid. The two sub-populations were found to be coeval within the errors and to differ mostly in metallicity. The use of other photometric filters can enhance the predictive power of this method (see contribution of Andrés Jordán in this volume). The maximum age resolution of this method at old ages (≥ 10 Gyr) can reach 2 – 3 Gyr and is strongly dependent on the photometric quality. This technique, however, is premised on the assumption that all sub-populations feature the same globular cluster mass function. On the other hand, if extended to a wider wavelength range this technique can be used to study variations in the globular cluster mass function. For example, accurate V and I photometry in NGC 4472 already allowed to constrain the variations in the mass characterizing the turn-over to be less than 20%.

2.2 Colour-Colour Method

Colour-colour diagrams offer an alternative approach to photometric ages without the assumption of same underlying globular cluster mass functions. Com-

bined with a wide wavelength coverage from the optical to the near-infrared, our group uses the two-colour diagram technique to derive relative ages of globular clusters in early-type galaxies (see contribution of Maren Hempel). The advantage of linking optical and near-infrared colours is that it reduces the age-metallicity degeneracy very efficiently. The reason for this is the enhanced metallicity sensitivity of optical/near-infrared colours (e.g. $V - K$) due to the sampling of metallicity-sensitive giant branch luminosity. At similar age-sensitivity as purely optical colours (e.g. $V - I$) this combination minimizes the age-metallicity degeneracy and increases the total age-sensitivity in a colour-colour diagram.

Figure 2 shows the results of an optical/near-infrared study of two nearby early-type galaxies, NGC 3115 and NGC 4365. Our group detected a significant population of intermediate-age globular clusters in NGC 4365 [8] which could not be detected from optical colours alone. The results were recently confirmed [5] with spectroscopic methods discussed below. Counterparts were also found in NGC 1316 [3] and NGC 5846 (see M. Hempel et al. in this volume). The subtle but important point of this study is the fact that an intermediate-age stellar population can be well-hidden in the diffuse light of galaxies. No hint for an intermediate-age stellar population in the diffuse light of NGC 4365 was found so far [1]. We clearly require more near-infrared data on globular cluster systems to quantify the mass fractions of such intermediate-age globular cluster sub-populations. Future work [4] could provide such numbers and strictly constrain the importance of certain galaxy formation scenarios.

3 Spectroscopic Age Dating

As in the photometric approach, spectroscopic ages are derived from the comparison of observed parameters with theoretical model predictions. A commonly-used tool is the so-called diagnostic plot in which a spectroscopic metallicity tracer is plotted against a spectroscopic age indicator. The best spectroscopic age indicators for old stellar populations are Balmer lines. However, there is still no ideal set or combination of spectroscopic parameters which are entirely free from the age-metallicity degeneracy. Yet, combined with a metallicity indicator which is almost independent of age robust estimates can be achieved. One way to measure the strength of Balmer lines in distant stellar populations is the use of spectroscopic indices which do not require high-resolution and high-S/N spectra. The Lick system [11] defines a number of such indices which are designed to measure the strength of three Balmer lines and many metal lines.

3.1 The relatively best Metallicity Indicator

Depending on the star formation history the chemical composition of a stellar population is subject to abundance variations, in particular the $[\alpha/\text{Fe}]$ ratio [12]. These variations blur the accuracy of any metallicity diagnostic. New SSP models for stellar populations with constant $[\alpha/\text{Fe}]$ ratio [10] allow to account for varying abundance ratios and to quantify the effect of changing

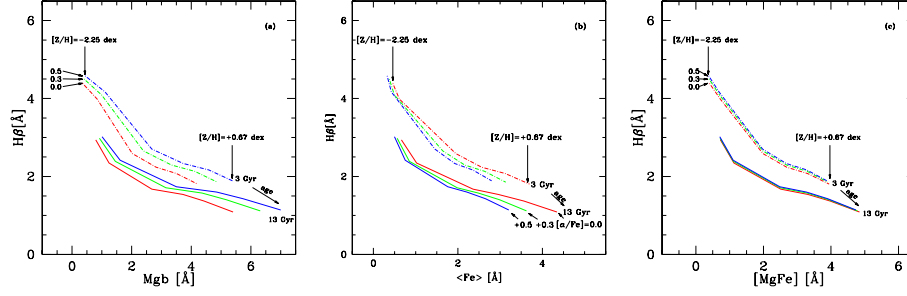


Fig. 3. Two iso-age lines (3 and 13 Gyr) are plotted as a function metallicity ($-2.25 \leq [Z/H] \leq +0.67$) parameterized for three $[\alpha/\text{Fe}]$ ratios (0.0, +0.3, and +0.5 dex) in three different diagnostic plots. (a): $H\beta$ vs. Mgb . The sensitivity to $[\alpha/\text{Fe}]$ can change the age prediction by up to ~ 5 Gyr. (b): $H\beta$ vs. $\langle \text{Fe} \rangle$. Sensitivity to $[\alpha/\text{Fe}]$ as in panel a. (c): $H\beta$ vs. $[\text{MgFe}]$. The isochrones in this diagnostic plot are least affected by $[\alpha/\text{Fe}]$ variations. Other Balmer line indices show similar behavior. The models are taken from [10]

$[\alpha/\text{Fe}]$ on spectroscopic indices. A good metallicity indicator can now be constructed with the requirement of being insensitive to abundance variations, but simultaneously trace the total metallicity. Gonzalez [2] found discrepant age predictions of theoretical models depending on the choice of Lick indices used as metallicity indicators. He speculated that this effect might be due to variation in the $[\alpha/\text{Fe}]$ ratio and could be cured by using the composite index $[\text{MgFe}] = \sqrt{Mgb \cdot (\text{Fe}5270 + \text{Fe}5335)/2}$. In Figure 3 the effects of changing $[\alpha/\text{Fe}]$ ratios on old and young isochrones are shown. Indeed, the composite index $[\text{MgFe}]$ is only little affected by abundance variations and should be used a metallicity indicator in all spectroscopic diagnostic plots.

3.2 The relatively best Age Indicator

The Lick system defines five Balmer line indices, $H\beta$, $H\gamma_A$, $H\gamma_F$, $H\delta_A$, and $H\delta_F$. The age sensitivity is different for each index and has never been quantified. Various combinations of Balmer indices and metallicity indicators are used in the literature and assigned equal importance. Here we define a quantity which can be used to determine the relatively best Lick Balmer-line index to age date stellar populations given the quality of data and any SSP model. The relative age-sensitivity of Balmer indices is a function of:

- η : mean error of the data
- ζ : transformation accuracy to the Lick system
- γ : mean error of the original Lick spectra
- δ : accuracy of the Lick fitting functions [13], [14]
- \mathcal{D}_Z : dynamic index range at a given metallicity
- $\mathcal{S}_{Z,t}$: sensitivity to age and metallicity at a given metallicity and age (i.e. the impact of the age-metallicity degeneracy)

Table 1. Summary of the coefficients in equation 2. Column 1 gives the mean data quality of the sample in Figure 4. The coefficients in columns 2-8 are given in units of Å. Columns 9-12 are given in dex/Gyr while the unit of \mathcal{R} in the last column is Å·dex/Gyr. The average dynamic age range \mathcal{D}_Z is evaluated at $[\text{Fe}/\text{H}] = -1.35$ and 0.0 between the 1 and 15 Gyr isochrone. \mathcal{S} is the mean of the degeneracies at two different metallicities $[\text{Fe}/\text{H}] = -1.35$ and 0.0 at two different ages 3 and 13 Gyrs.

	index η	ζ	γ	δ	$\langle \mathcal{D} \rangle$	$\langle \mathcal{S} \rangle$	\mathcal{R}
H β	0.60	0.232	0.22	1.30	2.62	0.274	0.488
H δ_A	0.79	1.043	0.64	1.27	7.42	0.147	0.565
H γ_A	0.82	0.722	0.48	1.78	9.38	0.166	0.723
H δ_F	0.83	0.790	0.40	1.18	4.15	0.130	0.318
H γ_F	0.84	0.448	0.33	1.34	5.19	0.136	0.421

where $\mathcal{S}_{Z,t}$, the degeneracy parameter, is

$$\mathcal{S}_{Z,t}(I) = \left. \frac{\partial I}{\partial t} \right|_Z \cdot \left(\left. \frac{\partial I}{\partial Z} \right|_t \right)^{-1}. \quad (1)$$

We define the quantity

$$\mathcal{R} = \frac{\mathcal{D}_Z \cdot \mathcal{S}_{Z,t}}{\sqrt{\eta^2 + \zeta^2 + \gamma^2 + \delta^2}} \quad (2)$$

which is maximal for the best age-sensitive index and is essentially the dynamic scale of an index I at a given age and metallicity expressed in units of the total uncertainty. Mean values of the dynamic range $\langle \mathcal{D} \rangle$ and the degeneracy parameter $\langle \mathcal{S} \rangle$ are used to evaluate \mathcal{R} . Both former parameters are derived from the SSP models of [6] and summarised in Table 1.

We find that from our data the relatively best age diagnostic is the H γ_A index followed by the indices H δ_A , H β , H γ_F , and H δ_F . If our data set were infinitely accurate (i.e. $\eta = 0$ in Eq. 2) the order of the Balmer-indices would remain the same. However, \mathcal{R} is subject to change when using different SSP models.

3.3 Spectroscopic Ages of Globular Clusters in Early-type Galaxies

First results of the age dating of globular clusters from our spectroscopic survey of globular cluster systems in early-type galaxies are shown in Figure 4. Independent of galaxy, metal-poor ($[\text{Fe}/\text{H}] < -0.8$) globular clusters appear to be old and coeval. Metal-rich ($[\text{Fe}/\text{H}] > -0.8$) globular clusters, on the other hand, cover a larger age range and appear on average younger. This interesting result indicates that metal-poor globular clusters might have preferentially formed very early, perhaps during or even before the assembly of their host galaxies. The metal-rich sub-population appears to form continuously until the recent

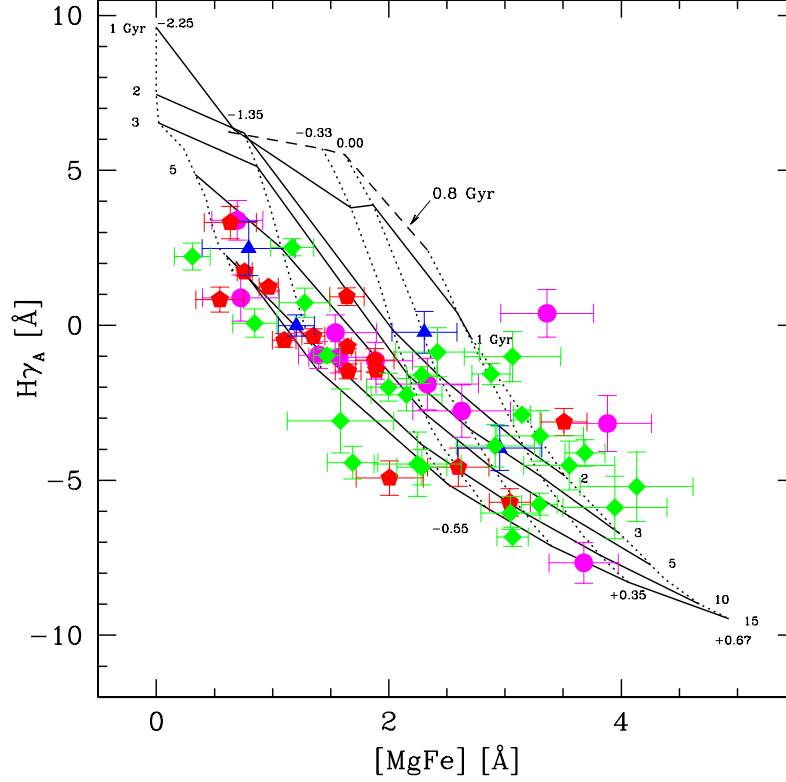


Fig. 4. Globular clusters in the early-type galaxies NGC 1380, NGC 2434, NGC 3115, and NGC 3379. SSP models were taken from [6]. Isochrones (*solid lines*) are plotted for the ages 1 to 15 Gyr. A very young iso-age line for a stellar population of 0.8 Gyr is also plotted (*dashed lines*). Iso-metallicity lines (*dotted lines*) are plotted for values $-2.25 \leq [Z/H] \leq +0.67$

past. This in turn implies that only the metal-rich population of clusters is augmented in later star formation events (see also M. Kissler-Patig et al. in this volume and [9]).

Some caveats have to be addressed when ages are derived from spectroscopic diagnostic plots. In the metal-poor regime ($[Fe/H] < -0.8$) at old ages ($t > 10$ Gyr), SSP model tracks start to overlap due to the increasing importance of hot blue horizontal branch stars. The consequence are ambiguous age predictions for old metal-poor populations and a potential age spread at old ages which cannot be ruled out. In the metal-rich regime ($[Fe/H] > -0.8$) the accurate age determination might also be hampered by an unknown contribution of the blue horizontal branch as a consequence of inaccurate modelling of the mass loss on the giant branch.

acknowledgements

It is a pleasure to thank my collaborators on various parts of this work Markus Kissler-Patig, Ralf Bender, Jean Brodie, Paul Goudfrooij, Maren Hempel, Michael Hilker, Claudia Maraston, Dante Minniti, Tom Richtler, Roberto Saglia, Daniel Thomas, and Steve Zepf. The financial support of the German *Deutsche Forschungsgemeinschaft*, *DFG*, under the grant number Be 1091/10–2 is gratefully acknowledged.

References

1. Davies, R. L. et al. 2001, *ApJL*, 548, L33
2. González, J. J. 1993, Ph.D. Thesis
3. Goudfrooij, P. et al. 2001, *MNRAS*, 328, 237
4. Hempel, M. et al. 2002, in preparation
5. Larsen, S.S., Brodie, J., Beasley, M., Forbes, D., Kissler-Patig, M., Kuntschner, H., Puzia, T.H. 2002, *ApJ* submitted
6. Maraston, C., Greggio, L., Renzini, A., Ortolani, S., Saglia, R.P., Puzia, T.H., & Kissler-Patig, M. 2002, *A&A* submitted, (astro-ph/0209220)
7. Puzia, T. H., Kissler-Patig, M., Brodie, J. P., & Huchra, J. P. 1999, *AJ*, 118, 2734
8. Puzia, T. H., Zepf, S. E., Kissler-Patig, M., Hilker, M., Minniti, D., & Goudfrooij, P. 2002a, *A&A*, 391, 453
9. Puzia, T. H., Kissler-Patig, M. et al. 2002b, *A&A* in preparation
10. Thomas, D., Maraston, C., & Bender, R. 2002, *MNRAS* submitted (astro-ph/0209250)
11. Trager, S. C., Worthey, G., Faber, S. M., Burstein, D., & Gonzalez, J. J. 1998, *ApJS*, 116, 1
12. Trager, S. C., Faber, S. M., Worthey, G., & González, J. J. ;. 2000, *AJ*, 119, 1645
13. Worthey, G., Faber, S. M., Gonzalez, J. J., & Burstein, D. 1994, *ApJS*, 94, 687
14. Worthey, G. & Ottaviani, D. L. 1997, *ApJS*, 111, 377